On the caveats of tracing molecular gas with CO emission

László Szűcs[1], Simon Glover[2], Ralf Klessen[2]

1) Max-Planck-Institut für extraterrestrische Physik 2) Zentrum für Astronomie Heidelberg, Institut für Theoretische Astrophysik

Introduction

The kinematics, masses and column densities of molecular clouds are fundamental parameters and indicators of star formation. These are often inferred from carbon monoxide (CO) isotope emission. A number of simplifications and assumptions, which can not be easily checked from observations, are involved in the inference methods.

We benchmark the most common methods and the underlying assumptions by applying them to emission maps of realistic hydrodynamic simulations (1, 2) and compare the inferred quantities to the true values. The simulations are analogues for low mass Milky Way molecular clouds. We explore the effects of metallicity, virial parameter, radiation field strength and cloud mass. Read our paper (3) for the discussion of the complete range and the detailed analysis.

Fig 1) A typical set of H_2 column density and ^{12}CO and ^{13}CO integrated emission maps used in the analysis (10^4 M⊙, solar metallicity, typical UV).

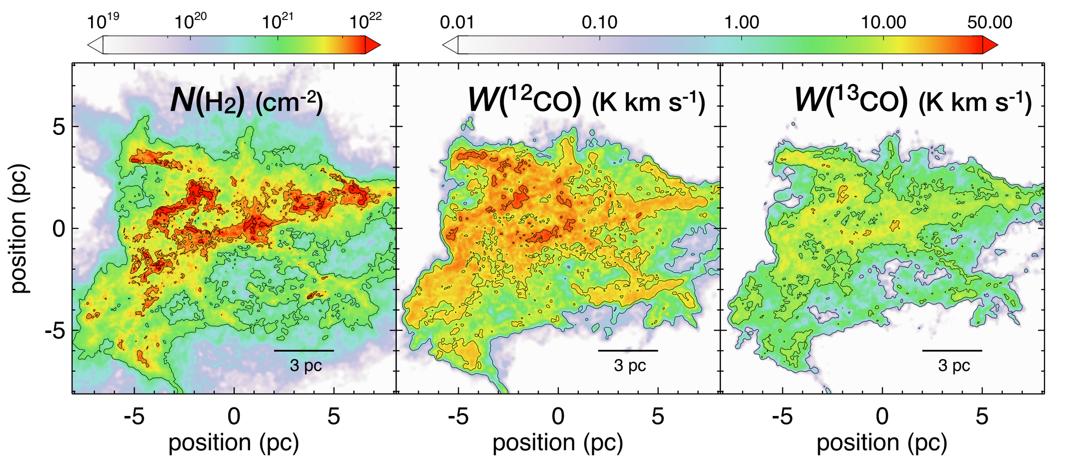

Inference methods

The tested CO emission based methods are: **a)** column density measurement of optically thin ^{13}CO, **b)** vital mass estimate and **c)** direct conversion of the emission to H_2 column density by the X_{CO}-factor. The principle steps are summarised in the bellow diagram:

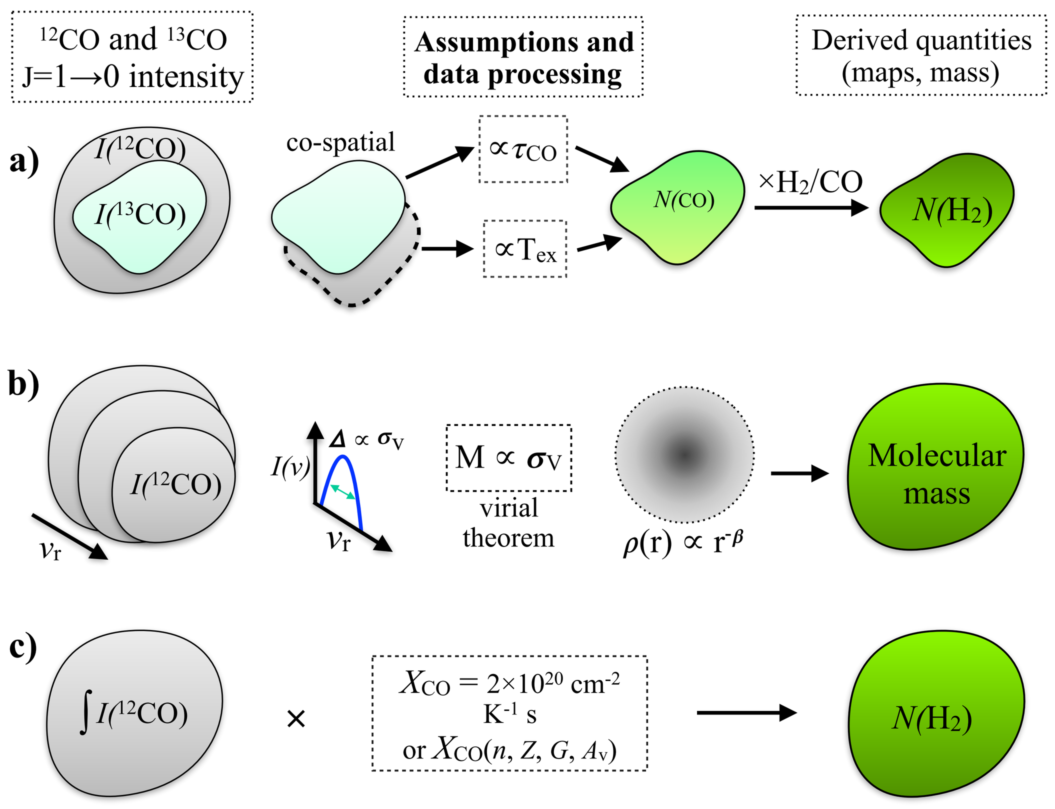

Brightness thresholds of 0.6 K and 0.3 K are applied to the ^{12}CO and ^{13}CO maps, respectively.

In (3) we compare a number of variants of the basic methods. The results for each are also shown here, but only the general trends are discussed.

Measured masses

The observed cloud mass ($M^{obs}_{>lim}$) is given by the integral of the inferred H_2 column density map. This is compared to the true H_2 mass (M^{H2}_{tot}) and the true H_2 mass above the CO brightness limits ($M^{sim}_{>lim}$). In the latter case we consider the mass above the ^{12}CO and ^{13}CO thresholds (#) and only above the ^{12}CO threshold (✻). The difference of (M^{H2}_{tot}) and ($M^{sim}_{>lim}$) is the CO dark molecular gas.

The observed to true mass ratios for several simulations and all methods❖ are compared in the bellow diagram:

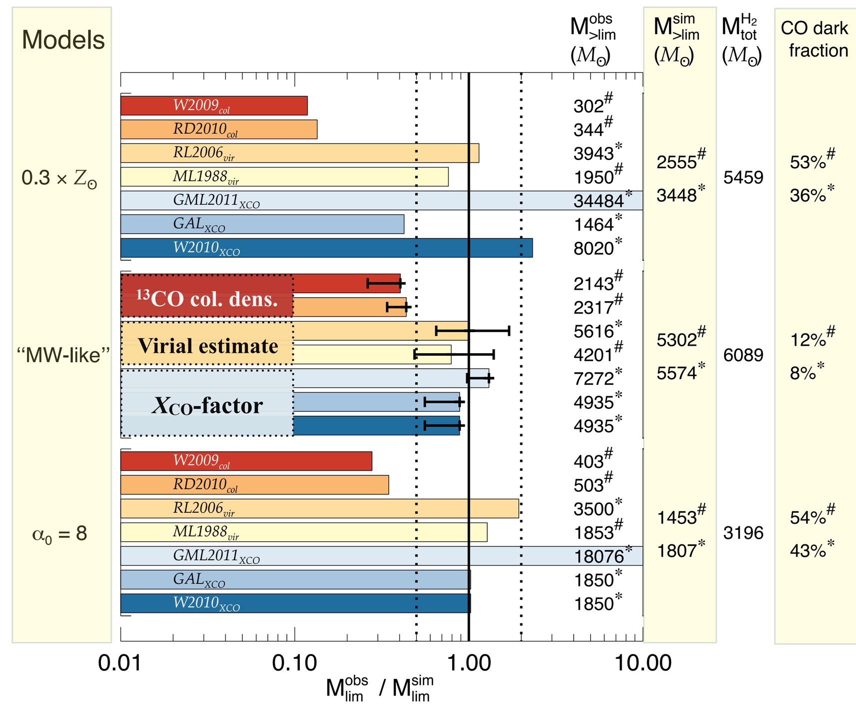

- ➤ CO column density methods systematically underestimate ($M^{sim}_{>lim}$).
- ➤ Virial methods are good indicators of the CO-bright mass, even when the cloud is super-virial.
- ➤ X_{CO} method is sensitive to the metallicity. The corrections might fail in some cases.

Column density of ^{13}CO

The comparison of the observed and the true column densities (**Fig. 2**) suggests that:

- ➤ H_2 column density inferred from the CO is shifted towards lower columns due to H_2/CO abundance ratio variations in the resolved cloud (compare dark grey and blue).
- ➤ The observed CO distribution does not follow the true CO distribution well (orange and blue) due to radiation transfer effects.

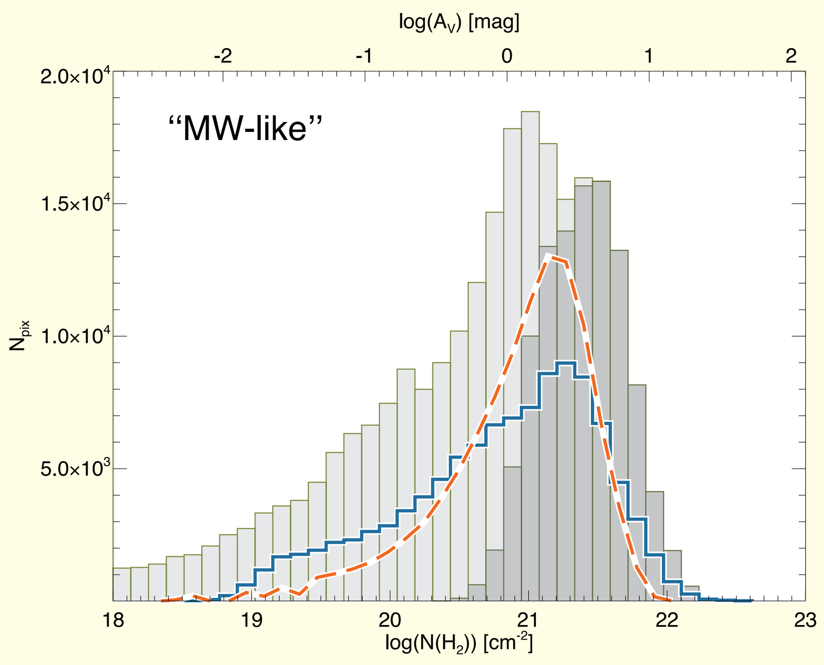

Fig 2) True H_2 column density (light grey), true H_2 above CO threshold (grey), true CO column density × H_2/CO (blue), inferred CO column density × H_2/CO (orange).

Why does the virial estimate work?

This method relies on three assumptions: the velocity dispersion is proportional to the CO line width, the radial density profile of the cloud follows a power law and the cloud is in virial equilibrium. We find that:

- ➤ The velocity dispersion can be recovered with 40 % error from the CO line width.
- ➤ **Fig. 3** shows that the radially averaged density distribution of several simulated clouds follow the assumed power law profile well.
- ➤ **Fig. 4** shows that the virial parameter of the CO bright gas is systematically lower than the virial parameter of the complete cloud, and tends towards the equilibrium value: CO might form where collapse is possible.

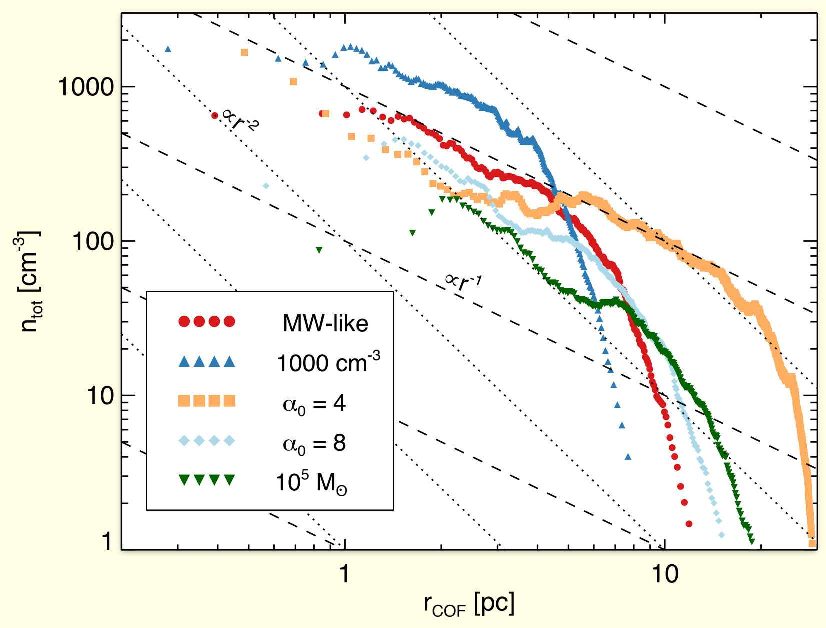

Fig 3) Radially averaged density profile of the simulated clouds. The dashed and dotted lines show the theoretical profiles.

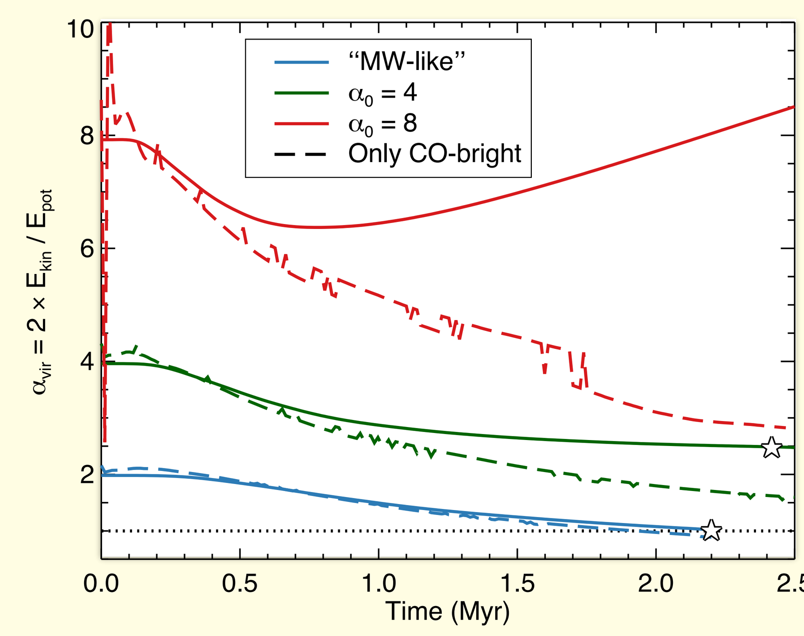

Fig 4) Virial parameter as a function of time. The solid line shows the complete cloud, while dashed only the CO-bright gas.

X_{CO} factor and mass estimate

It is widely accepted that the X_{CO}-factor breaks down on sub-parsec scales, and in fact it is recommended to be used on cloud averages. The behaviour of the cloud average X_{CO}-factor must, however, reflect systematics on sub-pc size scales (i.e. 0.03 pc × 0.03 pc). Thus on **Fig. 5** we show the pixel-wise X_{CO} factor as a function of visual extinction.

- ➤ Characteristic curve, with some dependence on physical conditions.
- ➤ Bimodal distribution, most pixel falls to ranges ② and ④.
- ➤ At low metallicity more pixels in range ②.

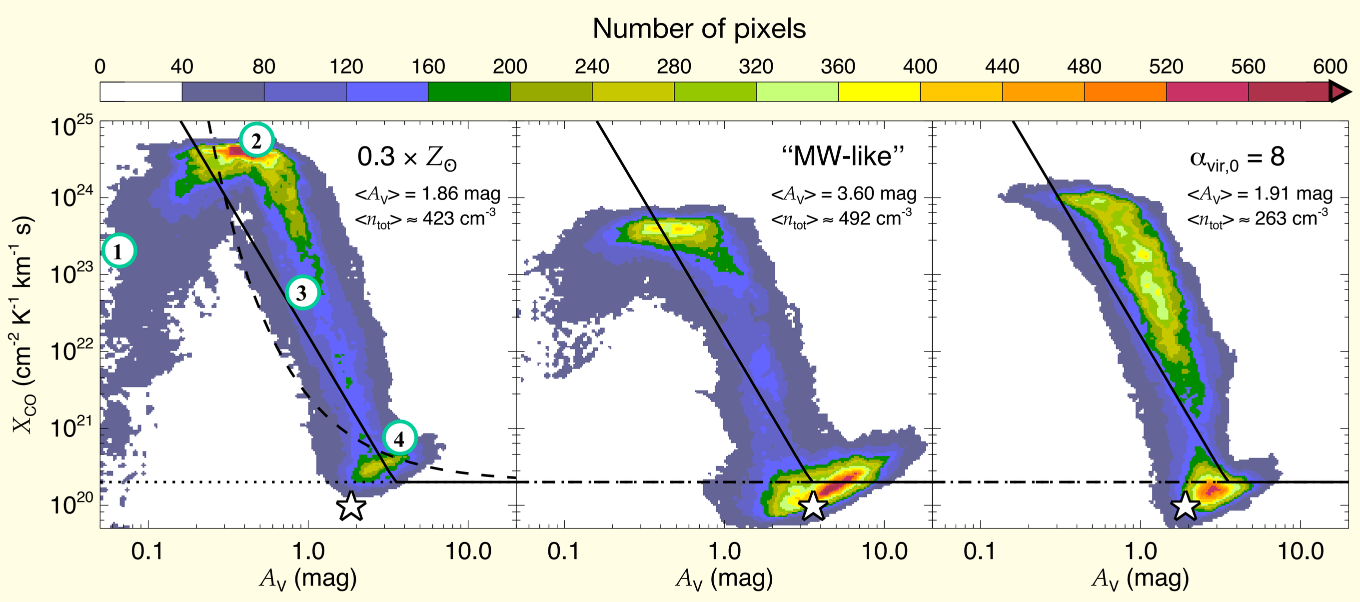

Fig 5) Pixel-wise X_{CO} factor as a function of visual extinction.

① Almost no CO, $N(H_2)$ increases quickly, CO shielded by H_2.
② Low A_V: little CO, H_2 and CO column grows together → constant ratio both CO and H_2 are dominantly shielded by dust.
③ Rapid decrease: sharp C^+ - C - CO transition.
④ Gradual increase: $N(H_2)$ increases, CO emission saturates.

Take home message

With the exception of the ^{13}CO column density measurement, all cloud mass inference methods recover the CO-bright H_2 mass within a factor of 2 uncertainty, if the metallicity is not too low.

- ➤ The ^{13}CO column density method if affected by chemical and optical depth issues and measures both the H_2 column density distribution and the molecular mass poorly.
- ➤ The virial mass is a good indicator of the H_2 cloud mass, even when the overall cloud is out of equilibrium. This is due to a systematically lower virial parameter in the CO emitting gas.
- ➤ A single X_{CO} factor seems a robust choice over a range of cloud conditions.

❖ ^{13}CO column density methods: W2009$_{col}$ (4), RD2010$_{col}$; virial methods: RL2006$_{vir}$ (5), ML1988$_{vir}$; X_{CO} methods: GML2011$_{XCO}$, GAL$_{XCO}$, W2010$_{XCO}$ (6). For the detailed description see (3).

MAX-PLANCK-GESELLSCHAFT
MPE
ZENTRUM FÜR ASTRONOMIE HEIDELBERG

References

(1) Glover & Clark 2012, MNRAS, 421, 9
(2) Szűcs, Glover & Klessen 2014, MNRAS, 445, 4055
(3) Szűcs, Glover & Klessen 2016, MNRAS, 460, 82
(4) Wilson et al. 2009, Tools of Radio Astronomy
(5) Rosolowsky & Leroy, 2006, PASP, 118, 590
(6) Wolfire et al. 2010, ApJ, 716, 1191

Acknowledgements

We acknowledge support from the Deutsche Forschungsgemeinschaft via SFB project 881 'The Milky Way System' and the European Research Council grant PALs (project number 108477). The numerical simulations were performed on the KOLOB cluster at the University of Heidelberg and on the MilkyWay supercomputer, funded by the DFG.

If you have any questions, comments or suggestions, then please feel free to ask me here or contact me at:

laszlo.szucs@mpe.mpg.de
https://ita.uni-heidelberg.de/~szucsl